Carbohydrate Polymers 85 (2011) 356–362

Contents lists available at ScienceDirect

Carbohydrate Polymers

journal homepage: www.elsevier.com/locate/carbpol

Visco-elastic properties of chitosan–titania nano-composites

F.A. Al-Sagheer*, S. Merchant

Department of Chemistry, Kuwait University, Faculty of Science, P.O. Box 5969, 13060 Safat, Kuwait

ARTICLE INFO

Article history:
Received 17 December 2010
Received in revised form 18 February 2011
Accepted 21 February 2011
Available online 25 February 2011

Keywords:
Nano-composites
Chitosan
Titania
Sol–gel
Visco-elastic properties

ABSTRACT

Chitosan–titania (Chitosan–TiO_2) nano-composites have been prepared via the sol–gel process. Tetraethylorthotitanate ($C_8H_{20}O_4Ti$) was used as a precursor to introduce titania network in the matrix. Different techniques have been used to characterize structure and morphology of the resulting hybrid. The inter-phase dynamics have been studied using dynamical mechanical thermal analysis (DMTA). Shift in glass transition (T_g) towards higher temperature, increased storage modulus and reduced loss modulus were observed on addition of titania in the matrix. The maximum value for storage modulus (6.7 GPa at 50 °C) and that of T_g at 160.9 °C was observed with 30 wt% of titania in the matrix. The improvement in the mechanical properties of the polymer was due to the homogeneous and ordered distribution of titania particles (5–25 nm) in the chitosan matrix resulting from the large interfacial interaction between the basic sites (NH_2) available on the polymer chains and Lewis acidic sites from titanium.

1. Introduction

The sol–gel process (Brinker & Scherer, 1990; Hench & West, 1990; Wen & Wilkes, 1996) is considered as a versatile route to prepare inorganic/organic hybrids under mild reaction conditions. The chemistry of the process involves hydrolysis and condensation of the alkoxides from different metals e.g., Si, Ti, Zr, etc. Depending upon the interfacial interaction the hybrids generated thus may exhibit a narrow distribution of particles, reduced particle size and enhanced mechanical, thermal, optical and morphological properties (Al Kandary, Ali, & Ahmad, 2005) overcoming the limitation posed by the individual components.

The development of bio-hybrid materials has become great interest in the recent years (Jancar et al., 2010). Chitosan is an attractive polymer particularly due to the amino and hydroxy functional groups present on its chain, which can be linked chemically to the inorganic reinforcing network in the hybrid preparation. The bio-degradability, non-toxicity and natural abundance of chitosan make it a green material which can be easily and economically extracted from marine canning industry byproducts (Al Sagheer, Al- Sughayer, Muslim, & Elsabee, 2009; Muzzarelli, 2010). It has attracted attention in the medical research community, for orthopedic applications (Muzzarelli, 2009, 2011) and the targeted drug delivery (Sokker, Abdel Gaffar, Gad, & Aly, 2009; Thomas, Dean, & Vohra, 2006) and as weight management supplement (Preuss, Bagchi, & Kaats, 2007; Sheilds, Smock, McQueen, & Bryant, 2003). The mechanical properties of the pure chitosan are, however, rather weak and may not be suitable for many other useful applications (Liu, Su, & Lai, 2004; Matsuda, Ikoma, Kobayashi, & Tanaka, 2004; Yang, Dou, Liang, & Shen, 2005; Zeng & Ruckenstein, 1996).

Quite recently the present authors have prepared chitosan–SiO_2 hybrids (Al Sagheer & Muslim, 2010) through the sol–gel process and have shown that silica reinforcement in the matrix improves thermal and mechanical properties over the pure polymer. The major drawback, however, with chitosan–silica hybrids is silica's hydrolytic instability (Brunel et al., 2003), especially under the basic conditions and absence of any functionality except the surface hydroxyl groups. The use of titania instead of silica could circumvent these problems as titania shows better hydrolytic stability under the basic conditions. Titanium dioxide (TiO_2) has been used extensively as a reinforcement material (Ahmad, Sarwar, & Mark, 1998; Chen & Mao, 2007; El Kadib, Molvinger, Bousmina, & Brunal, 2010; Hu, Ge, Sun, Zhang, & Yin, 2007; Sarwar, Zulfiqar, & Ahmad, 2007) of choice due to its low price, chemical stability, photo-catalytic activity, good optical transparency besides its anti-bacterial properties (Sadiq, Chandrasekharan, & Mukherjee, 2010). Chitosan–TiO_2 membranes (Yang, Li, Jiang, Lu, & Chen, 2009) were prepared by the sol–gel processing using tetrabutyl titanate. Acetylacetone was used as chelating agent to control the sol–gel reaction leading to titania formation. The nano-sized titania particles were distributed homogeneously within the chitosan matrix. The hybrid membranes showed better pervaporation performance for ethanol dehydration. Highly active/selective catalyst hybrid materials based on chitosan–TiO_2 featuring high surface area have been prepared by El Kadib, Molvinger, Guimon, Quignard, and

* Corresponding author. Tel.: +965 24987076; fax: +965 24816482.
E-mail addresses: f.alsagheer@ku.edu.kw, faalsagheer@hotmail.com (F.A. Al-Sagheer).

0144-8617/$ – see front matter © 2011 Elsevier Ltd. All rights reserved.
doi:10.1016/j.carbpol.2011.02.032

Brunal (2008). Improvement in thermal and mechanical properties of chitosan–TiO_2 can play an important role in the application of such hybrid membranes and support catalysts. The compatibility of the hydroxyl and amine group of chitosan with titanium ethoxide to develop an in situ titania network via the sol–gel process can give spatially well distributed nano-phase titania in chitosan matrix which can improve the thermal and mechanical properties of chitosan significantly. Such studies on chitosan–TiO_2 have been scarce especially with regards to the variation in its viscoelastic properties and their dependence on the composition of the inorganic network.

In the present work we describe the synthesis of chitosan–TiO_2 composites with varying titania contents through the sol–gel process. The analysis of thermo-mechanical properties as a result of polymer modification has been carried out by the DMTA (dynamical mechanical thermal analysis). The information related to the stress–strain behavior during deformation, molecular and segmental motion of the polymer matrix in the glassy or rubbery regions has been obtained as it is subjected to temperature variation. Temperature dependence of tan δ gave a measure of the glass transition temperature (T_g) of the hybrid materials. Their modified morphology has been studied through SEM to show the nature of the nanophase titania particles and their distribution in the matrix.

2. Methods

2.1. Materials

Practical grade of Chitosan with Brookfield viscosity >200.00 cps was obtained from Aldrich and used as received. Tetraethylorthotitanate obtained from Gelest Inc with purity 95% was used as received. Glacial acetic acid (100%) obtained from Merck was used with deionized water to dissolve the polymer.

2.2. Preparation of the hybrid films

Chitosan polymer solution (2 wt%) was prepared by dissolving it in acetic acid (as 2 wt% solution in deionized water). This solution was stirred for 48 h at room temperature to form a homogenous solution. A required amount of this solution was taken in a 50 ml bottle and a measured amount of tetraethylorthotitanate was added to it. This was stirred for 1 h at room temperature. A stoichiometric amount of water (water:tetraethylorthotitanate mol ratio kept as 1:1.5) was added through a solution containing an equimolar mixture of ethanol and water and the mixture was allowed to stir for 18 h at room temperature to carry out the sol–gel process. This solution was then cast in Teflon petri dishes to obtain thin hybrid film through solvent elution. These hybrid films with varying ratio of titania (from 5 to 30 wt%) in the matrix were dried at 50 °C for 18 h and kept under vacuum for another 48 h at 50 °C for complete removal of the solvent.

2.3. Analysis of the hybrid films

FTIR spectroscopic analysis was carried out on Perkin-Elmer FTIR-2000 spectrophotometer. Morphology of the hybrid films was studied using field emission scanning electron microscope model Leo Supra 50VP FE-SEM. The films were brittle-fractured, sputter coated with gold by means of Balzer's SCD-050 and mounted on aluminum before analysis. Elemental X-ray microanalysis was conducted on a JSM-6300-J scanning electron microscope attached to an energy dispersive X-ray spectroscope operated at 20 kV for analyzing the specimens. The electron beam penetrates 2–3 μm below the surface of the chitosan sample to highlight the underlying titania distribution. For measurement of the size of sol–gel produced particles the hybrid samples with 5 and 10% titania loading were degraded at 430 °C for 9 h to decompose the organic matrix,

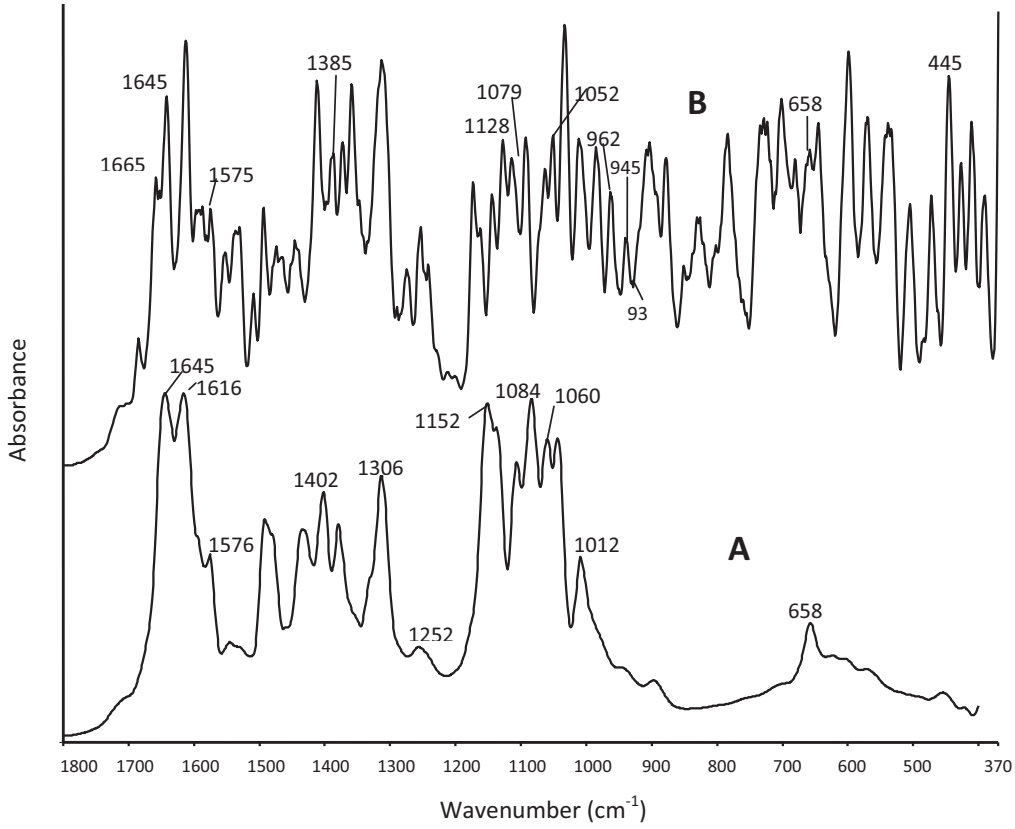

Fig. 1. FTIR spectra (370–1800 cm^{-1}) for: pristine chitosan (A); chitosan–TiO_2 hybrid with 20 wt% titania (B).

prior to imaging by the JEOL's microscope HRTEM-3010 which was equipped with a 300 kV electron gun. Surface topography was analyzed via the AFM using Nanoscope-IV multimode atomic force microscope.

The DMTA on the hybrid films was carried out using DMA Q-800 (TA, USA). The measurement of storage modulus and tan δ was carried out under tension mode in the temperature range 50–210 °C at a heating rate of 2 °C/min using a frequency of 2 Hz under inert atmosphere. Chitosan hybrid samples with varying titania contents with a rectangular geometry were mounted on the clamps and subjected to sinusoidal stress at various temperatures. The consequent sample strain proportional to its displacement was measured by the instrument. The T_g was measured from the maxima of the tan δ versus temperature curves.

3. Results and discussion

3.1. FTIR spectroscopy

Fig. 1 compares the FTIR spectra of pristine chitosan with the chitosan–TiO_2 hybrid film containing 20% titania in the range 400–2000 cm^{-1}. The amide bonds in chitosan in the spectrum (A) show the characteristic absorbance at 1645 cm^{-1} due to stretching of amide I (C=O) and bending due to amide II (N–H) at 1616 cm^{-1} (Zeng & Ruckenstein, 1996). The absorbance band at 1576 cm^{-1} corresponds to the interaction of γ(C–N) and δ(C–N–H). The C–H bond interaction due to amide II is indicated at 1306 cm^{-1} and 1402 cm^{-1}. The absorption at 1252 cm^{-1} is characteristic of secondary amides and the band at 658 cm^{-1} is due to the δ(N–H) wagging, whereas the peak at 1152 cm^{-1} shows anti-symmetric C–O–C stretching (Martinez, Retuert, Yezdani-Pedram, & Colfen, 2004). The bands depicting the skeletal stretch of C–O in polysaccharides are evident at 1012 cm^{-1}, 1060 cm^{-1} and 1084 cm^{-1} (Martinez et al., 2004). In contrast to the pure chitosan film, the spectrum B for chitosan–TiO_2 hybrid film shows a new region of absorption between 400 and 800 cm^{-1} depicting the Ti–O–Ti network formation (Yang et al., 2009). The presence of titania network is seen through with the growth of a band at 455 cm^{-1} which is ascribed to the Ti–O, that is absent in the pure chitosan showing incorporation of titania via the sol–gel method. Some un-condensed but hydrolyzed titanium alkoxide is seen as the Ti-OH groups showing peaks at 1665 cm^{-1} where as some unhydrolyzed alkoxy groups also give their appearance at 1079 cm^{-1} and 1128 cm^{-1} (Sarwar et al., 2007). The evidence of inter-phase compatibility is seen from the appearance of bands at 962 cm^{-1} and 945 cm^{-1} showing the interaction of Ti Lewis sites with the NH_2 groups from chitosan chain (Gianotti et al., 2002). The hydroxyl groups of the hydrolyzed TEOT during the sol–gel process can also condense with the –OH groups on the chitosan chain thus creating a chemical bond between the organic and inorganic phase. As a result the creation of Ti–O–C bond through such chemical interaction in the hybrid film is seen at 1128 cm^{-1} and 1052 cm^{-1} (Hu et al., 2007; Yang et al., 2009).

Fig. 2 shows a comparison of the FTIR spectra of pure chitosan and the chitosan–TiO_2 hybrid film in the range of 3000–3800 cm^{-1}. The ν(OH) and δ(N–H) bands from the chitosan polymer are seen at 3424 cm^{-1} and 3285 cm^{-1} respectively. The influence of matrix modification and interfacial interaction between the organic and inorganic phases is evident due to the overall reduction in intensity in the amide regions and the shift of this band to lower frequency whereas the peak of 3424 cm^{-1} becomes wider, indicating the hydrogen bonding. The bands appearing in the region from 3568 to 3721 cm^{-1} which are absent in the pure chitosan sample are described due to hydroxyl groups attached to titania network (Gianotti et al., 2002). The influence of matrix modification by the titania network is also seen by the overlapping of OH and NH stretching in the 3337–3374 cm^{-1} region whereas the pure chitosan film show clear band at 3330 cm^{-1} due to asymmetric stretching of NH_2 in the polymer chain. This region also marks the effect of hydrogen bonding between chitosan and the inorganic network. The attractive polymer–particle interactions between chitosan and titania through primary and secondary bonds as depicted

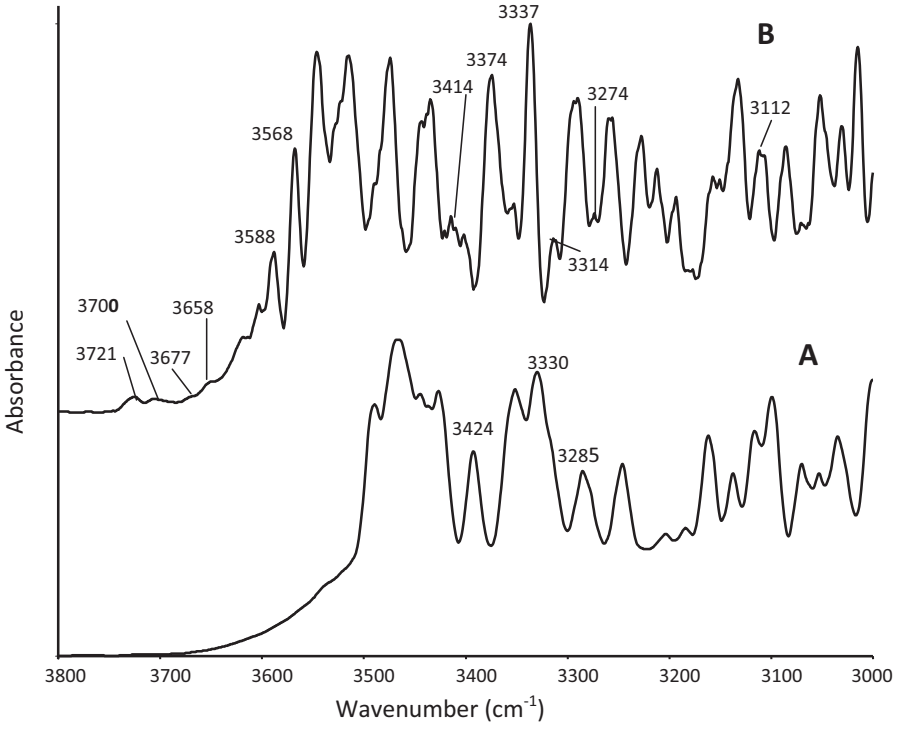

Fig. 2. FTIR spectra (3000–3800 cm^{-1}) for: pristine chitosan (A); chitosan–TiO_2 hybrid with 20 wt% titania (B).

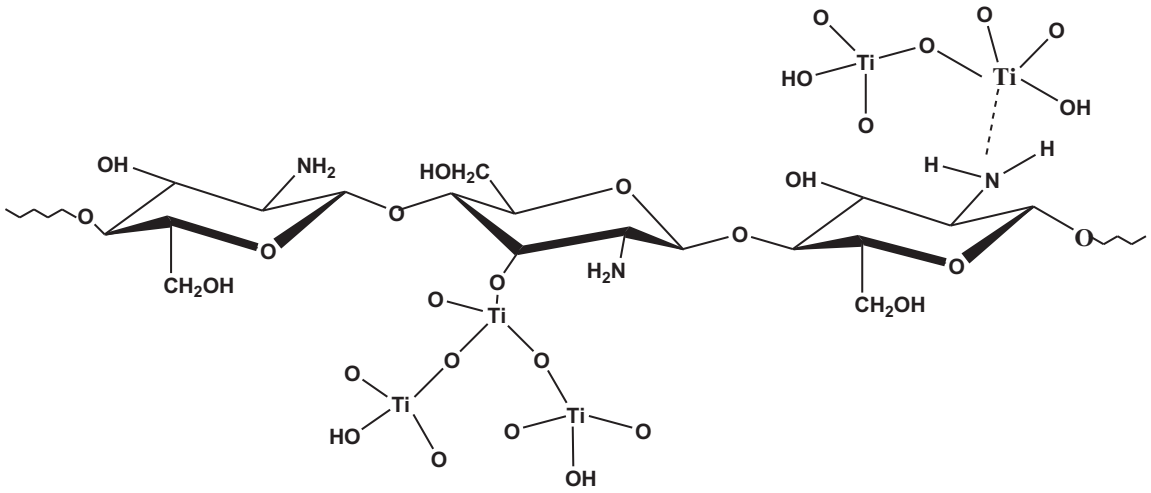

Fig. 3. Chemical and physical interactions between titanium network and chitosan chain.

in Fig. 3 can help greatly to reduce the agglomeration tendencies of the inorganic network in the matrix which can have positive effect on the properties of the hybrids.

3.2. Morphological studies

Field emission scanning electron spectroscope (FESEM) was used to analyze the morphology of the chitosan–TiO_2 hybrids carried out on their fractured films. These micrographs for the hybrids with 10 and 20 wt% of titania are shown in Fig. 4. The particles appear as dense phase in the form of white round beads having slightly diffused surface. The blurred surface indicates adsorption of the polymer layers on the particle surface. The uniform dispersion of spherical particles is the outcome of spinodal decomposition (Inoue, 1995) process that takes place during drying at higher temperature condensation stage. Elemental X-ray mapping for the chitosan hybrid films with 5 and 20 wt% of titania is shown in Fig. 5. It shows a well dispersed nano-sized distribution of inorganic network in the chitosan matrix. For measurement of the sol–gel produced particle size the hybrid samples with 5 and 10 wt% titania were degraded at 430 °C for 9 h to decompose the organic matrix, prior to imaging by TEM. Fig. 6 confirms the size of nanoparticles ranging from 5 to 25 nm was achieved in these hybrids. This demonstrates the effective application of the sol–gel process towards preparing these nano-composites. Surface topography of the pure matrix and its hybrids with 10 and 20 wt% of titania giving information about surface roughness and texture is shown in Fig. 7. The surface of the pure chitosan film (A) is porous and regular as the polymer matrix shows minor undulations of the chains per se. The polymer matrix surrounds the particle in the hybrids showing irregular surface topography. The inorganic particles are covered like a blanket by the polymer chains and at lower titania

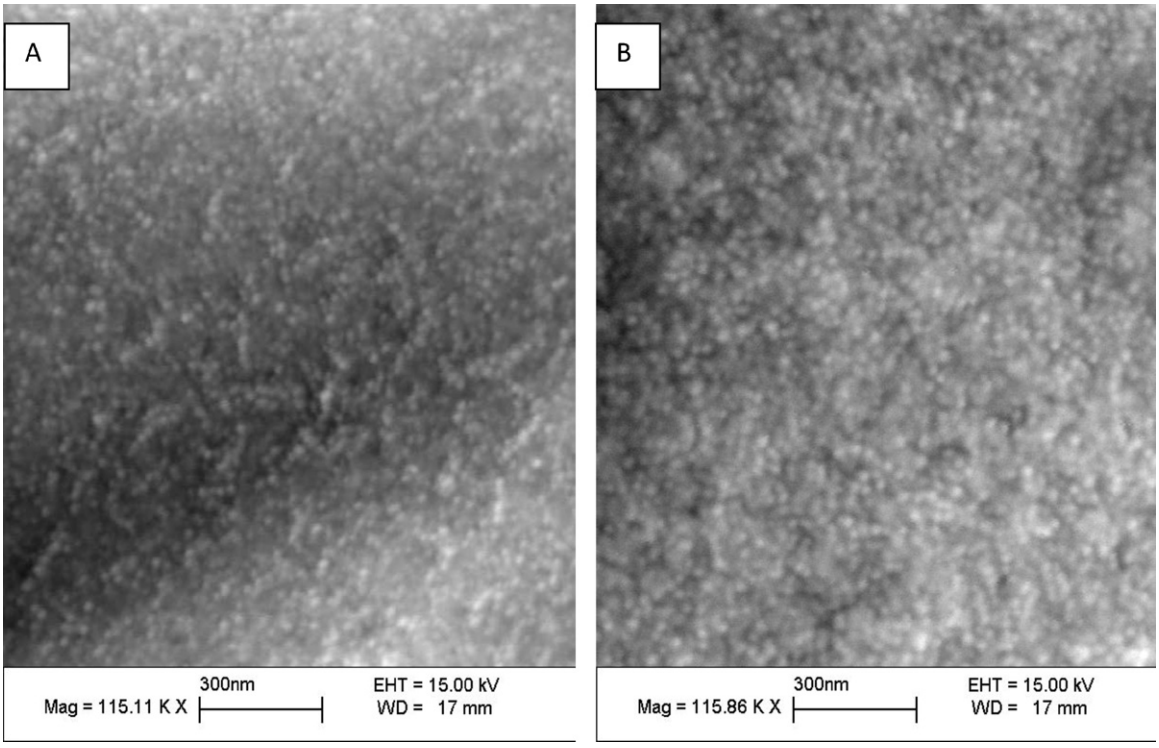

Fig. 4. High magnification FE-SEM images of chitosan–TiO_2 hybrids with titania contents wt%: 10 (A) and 20 (B).

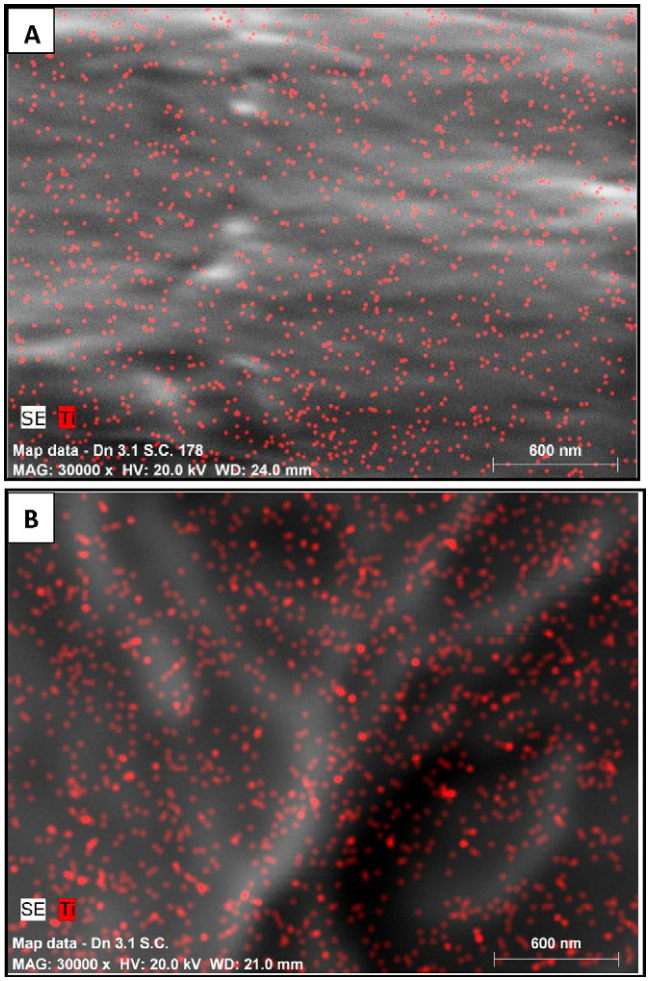

Fig. 5. Elemental X-ray mapping images of chitosan–TiO_2 hybrids with titania wt%: 5 (A) and 20 (B).

content the elevation contour size is of nearly 125 nm with deeper areas, where there are few or no particles. As the amount of titania is increased, the polymer surface is superficially undulated to show few big contours of nearly 300 nm in diameter. As the dense distribution of particles is engulfed by the polymer chains, the image shows a fine and smoothly undulated surface topography where the titania network itself has aligned itself with the polymer chains.

Relatively smaller size and uniform dispersion of contours point to specific role of coupling due to the secondary and primary bond interactions between inorganic and organic phases thus controlling the morphology and distribution of the inorganic component. These results compliment the morphological results observed from SEM and TEM and FTIR analyses.

3.3. Visco-elastic properties

Fig. 8 shows the variation of storage modulus of pure chitosan and its hybrids with temperature. The storage modulus reveals the ability of the material to resist deformation and store mechanical energy. The modulus value of 3.67 GPa was observed for pure chitosan at 50 °C. This region at lower temperature is the glassy phase where the molecular motions of chitosan are largely restricted to the vibration and short-range rotational motions of bond bending or bond angle deformation. The second region is transitional between the glassy and the rubbery region where the side chain and main chain rotation becomes evident with increasing temperature. Here the modulus shows a linear drop between 110 °C and 150 °C. In the visco-elastic region the deformation is reversible and time-dependent marking the glass transition temperature. The slight increase in modulus between 180 and 210 °C may be due to the rapid alignment of the polymer chains under sinusoidal stress or some cross-linking within the chains thus raising the storage modulus once again in the post glass transition region.

The storage modulus for the hybrid films with 5, 10, 20 and 30 wt% of titania increases with increasing titania content and reaches to the maximum at 6.7 GPa for chitosan–TiO_2 30% at 50 °C. Below T_g increase in modulus was almost 80% as compared to pure chitosan. Above T_g the storage modulus is enhanced by 143% from 1.63 GPa in the unmodified matrix to 3.9 GPa for the chitosan–TiO_2-30%. At the same time the linear decrease in modulus with temperature for pure chitosan from 3.67 GPa to 1.626 GPa is 124% whereas the decrease in modulus with temperature for chitosan–TiO_2-30% is only 69%. The visco-elastic relaxations in the hybrids depend on the bonding between the polymer–particle interfaces. These interactions play a key role in controlling the local dynamics of the polymer/particle mixture (Ahmad et al., 1998).

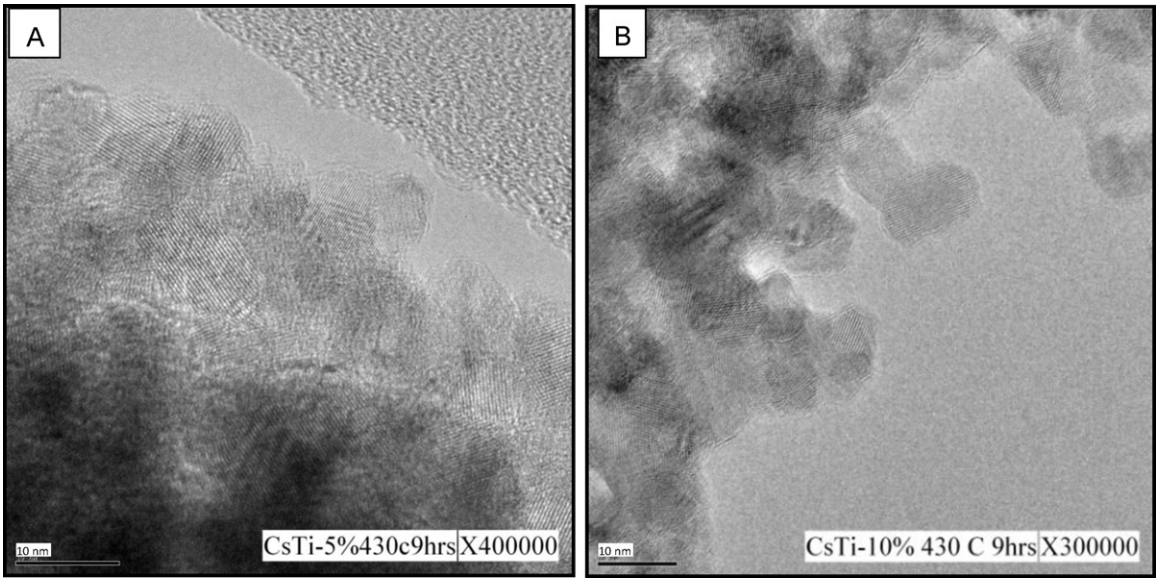

Fig. 6. High resolution transmission electron microscopy images showing the individual particle size for the chitosan–TiO_2 hybrids with titania wt%: 5 (A) and 10 (B).

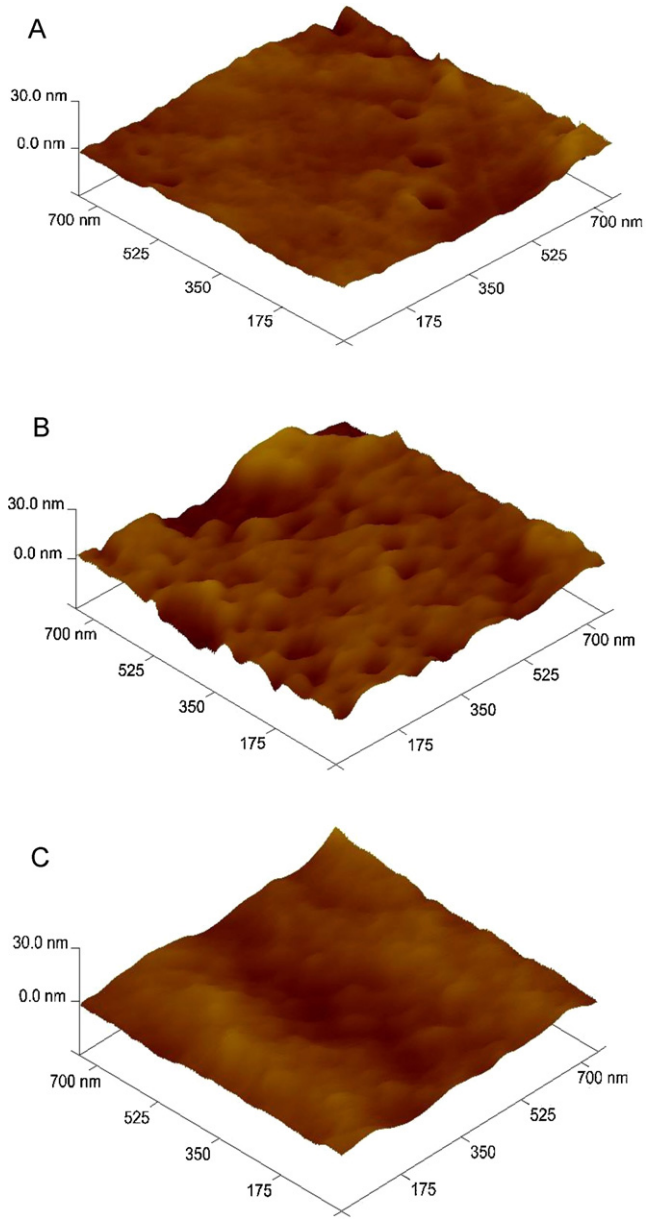

Fig. 7. Atomic force microscopy topographs of chitosan–TiO_2 hybrids with titania wt%: 0 (A); 10 (B); and 20(C).

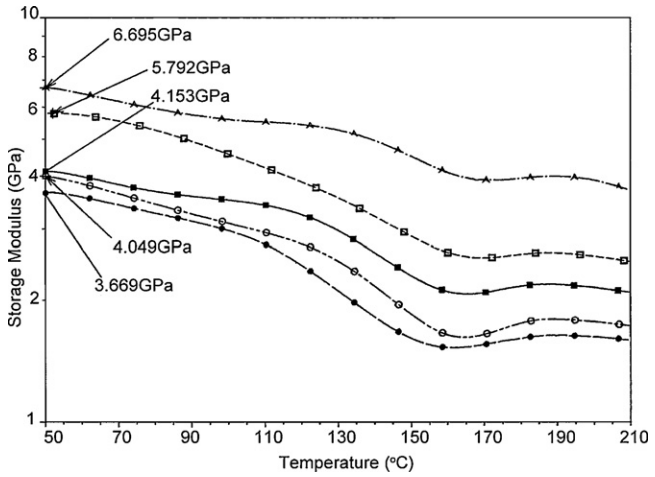

Fig. 8. Temperature variation of storage modulus for chitosan–TiO_2 hybrids at 2 Hz. Titania wt%: 0 (●), 5 (o), 10 (■), 20 (□), and 30 (⮝).

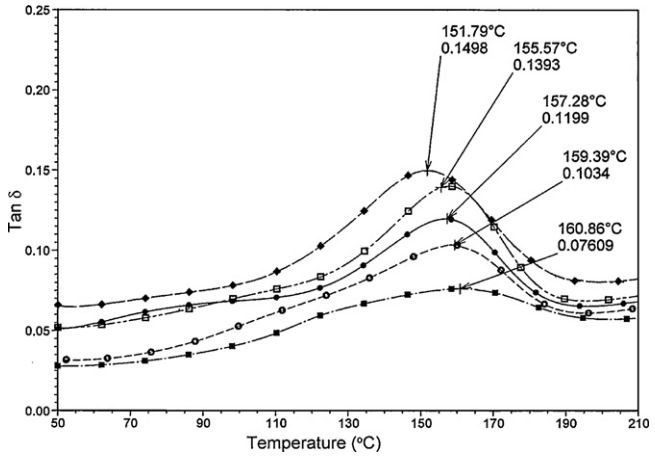

Fig. 9. Temperature variation of tan δ for chitosan–TiO_2 hybrids at 2 Hz. Titania wt%: 0 (♦), 5 (□), 10 (●), 20 (◯), and 30 (■).

Nano-fillers due to large surface interaction slow down greatly the segmental dynamics of the polymer which shows a high retention of modulus at higher temperature. The effect of covalent/hydrogen bonding will lead further to reduction in segmental motion which is also reflected in a shift in the T_g.

Fig. 9 shows the variation of tan δ with temperature for the pure chitosan and its hybrid films. The peak of these curves represents the T_g due to α-relaxations involving large segmental motions. The reduce area under the peak or damping denotes the stiffness in the polymer. In pure chitosan, this peak is marked at 151.79 °C. The pure polymer shows the highest peak as it dissipates more energy applied to the sample due to its viscous response at high temperature. As titania content is increased the mobility of the chains is suppressed due to the attractive particle–polymer interactions. The highest recorded glass transition temperature for this system was seen for the CSTi-30% at 160.86 °C which shows an increase of 9 °C from the pristine chitosan matrix. The shift in glass transition to higher temperature is indicative of reduced segmental motion due to homogenously distributed titania nano-particles requiring greater thermal energy for the transition to occur. As the amount of titanium increases the shift is expected to be greater but the particle size also increases in proportion, reducing the surface interaction and thus showing a relatively lower increment in T_g at a higher concentrations of titania. The cross-link density of the nonlinear inorganic network and its interaction increases the damping effect thus reducing the tan δ peak as well as broadening it. The pure polymer had a tan δ value of 0.15. The highest damping or elasticity is seen in the chitosan–TiO_2-30% at 0.076 where there is a direct relation between stiffening of the hybrids to titania composition due to increased interfacial interaction of the inorganic phase through bonding with the functional groups present on the organic polymer.

4. Conclusions

Sol–gel chemistry has been employed to prepare the chitosan–titania oxide hybrids. The interfacial interaction between the organic and inorganic phases resulted in a nano-scale (5–25 nm) dispersion of titania in the matrix which has improved greatly the glass transition temperature and the modulus of the matrix. Such chitosan hybrids with improved thermal and mechanical properties can be very useful as support catalyst and hydrolytically stable polymer membranes.

Acknowledgements

The authors wish to acknowledge the financial support provided by the Kuwait University under the project SC02/06. They would also like to appreciate the technical support from the E.M unit and the general facilities projects GS01/01, GS01/05 under the SAF program. They also acknowledge the gracious support and contribution made by Prof. Zahoor Ahmad from the Chemistry Department of Kuwait University.

References

Ahmad, Z., Sarwar, M. I., & Mark, J. E. (1998). Thermal and mechanical properties of aramid-based titania hybrid composites. *Journal of Applied Polymer Science*, *70*, 297–302.

Al Kandary, Sh., Ali, A. A. M., & Ahmad, Z. (2005). Morphology and thermo-mechanical properties of compatibilized polyimide–silica nanocomposites. *Journal of Applied Polymer Science*, *98*(6), 2521–2531.

Al Sagheer, F. A., Al-Sughayer, M. A., Muslim, S., & Elsabee, M. Z. (2009). Extraction and characterization of chitin and chitosan from marine sources in Arabian Gulf. *Carbohydrate Polymers*, *77*(2), 410–419.

Al Sagheer, F. A., & Muslim, S. (2010). Thermal and mechanical properties of chitosan/SiO_2. Hybrid composites. *Journal of Nano-Materials*, 7. Article id 490679.

Brinker, C. J., & Scherer, G. W. (Eds.). (1990). *Sol–gel science: The physics and chemistry of sol–gel processing*. New York: Academic Press.

Brunel, D., Blanc, A. C., Mutin, P.-H., Lorret, O., Lafond, V., Galarneau, A., et al. (2003). Design of supported catalysts by surface functionalization of micelle-templated silicas. *Studies in Surface Science and Catalysis*, *146*, 419–425.

Chen, X., & Mao, S. S. (2007). Titanium dioxide nanomaterials: Synthesis, properties, modifications, and applications. *Chemical Reviews*, *107*, 2891–2959.

El Kadib, A. E., Molvinger, K., Bousmina, M., & Brunal, D. (2010). Improving catalytic activity by synergic effect between base and acid pairs in hierarchically porous chitosan@titania nanoreactors. *Organic Letters*, *12*, 948–951.

El Kadib, A. E., Molvinger, K., Guimon, C., Quignard, F., & Brunal, D. (2008). Design of stable nanoporous hybrid chitosan/titania as cooperative bifunctional catalysts. *Chemistry of Materials*, *20*, 2198–2240.

Gianotti, E., Dellarocca, V., Marchese, L., Martra, G., Coluccia, S., & Maschmayer, T. (2002). NH_3 adsorption on MCM-41 and Ti-grafted MCM-41. FTIR, DR UV–Vis–NIR and photoluminescence studies. *Physical Chemistry Chemical Physics*, *4*, 6109–6115.

Hench, L. L., & West, J. K. (1990). The sol–gel process. *Chemical Reviews*, *90*, 33–72.

Hu, Y., Ge, J., Sun, Y., Zhang, T., & Yin, Y. (2007). A self-templated approach to TiO_2 microcapsules. *Nano Letters*, *7*, 1832–1836.

Inoue, T. (1995). Reaction-induced phase decomposition in polymer blends. *Progress in Polymer Science*, *20*, 119–153.

Jancar, J., Douglas, J. F., Starr, F. W., Kumar, S. K., Cassagnau, P., Lesser, A. J., et al. (2010). Current issues in research on structure–property relationships in polymer nanocomposites. *Polymer*, *51*, 3321–3343.

Liu, Y. L., Su, Y. H., & Lai, J. Y. (2004). In situ crosslinking of chitosan and formation of chitosan silica hybrid membranes with using gamma-glycidoxypropyltrimethoxysilane as a crosslinking agent. *Polymer*, *45*(20), 6831–6837.

Martinez, Y., Retuert, J., Yezdani-Pedram, M., & Colfen, H. (2004). Hybrid ternary organic–inorganic films based on interpolymer complexes and silica. *Polymer*, *45*, 3257–3265.

Matsuda, A., Ikoma, T., Kobayashi, H., & Tanaka, J. (2004). Preparation and mechanical property of core-shell type chitosan/calcium phosphate composite fiber. *Materials Science and Engineering*, *24*, 723–728.

Muzzarelli, R. A. A. (2011). Chitosan composites with inorganics, morphogenetics proteins and stem cells, for bone regeneration. *Carbohydrate Polymers*, *83*, 1433–1445.

Muzzarelli, R. A. A. (2010). Chitins and chitosans as immuneadjuvants and non-allergenic drug carriers. *Marine Drugs*, *8*, 292–312.

Muzzarelli, R. A. A. (2009). Chitins and chitosans for the repair of wounded skin, nerve, cartilage and bone. *Carbohydrate Polymers*, *76*, 167–182.

Preuss, H. G., Bagchi, D., & Kaats, G. R. (2007). Laboratory and clinical studies of chitosan. In D. Bagchi, & H. G. Preuss (Eds.), *Obesity: Epidemiology, pathophysiology, and prevention* (pp. 413–421). London: CRC Press.

Sadiq, I. M., Chandrasekharan, N., & Mukherjee, A. (2010). Studies on effect of TiO_2 nanoparticles on growth and membrane permeability of *Escherichia coli*, *Pseudomonas aeruginosa*, and *Bacillus subtilis*. *Current Nanoscience*, *6*(4), 81–387.

Sarwar, M., Zulfiqar, S., & Ahmad, Z. (2007). Preparation and properties of polyamide–titania nanocomposites. *Journal of Sol–Gel Science and Technology*, *44*, 41–46.

Sheilds, K. M., Smock, N., McQueen, C. E., & Bryant, P. (2003). *American Journal of Health System Pharmacy: AJHP: Official Journal of the American Society of Health System Pharmacists*, *60*(13), 1310–1312, 1315–1316.

Sokker, H. H., Abdel Gaffar, A. M., Gad, Y. H., & Aly, A. S. (2009). Synthesis and characterization of hydrogels based on grafted chitosan for the controlled drug release. *Carbohydrate Polymers*, *75*, 222–229.

Thomas, V., Dean, D. R., & Vohra, Y. K. (2006). Nanostructured biomaterials for regenerative medicine. *Current Nanoscience*, *2*(3), 155–177.

Wen, J., & Wilkes, G. L. (1996). Organic/inorganic hybrid network materials by the sol–gel approach. *Chemistry of Materials*, *8*(8), 1667–1681.

Yang, D., Li, J., Jiang, Z., Lu, L., & Chen, X. (2009). Chitosan/TiO_2 nanocomposite pervaporation membranes for ethanol dehydration. *Chemical Engineering Science*, *64*, 3130–3137.

Yang, Q., Dou, F., Liang, B., & Shen, Q. (2005). Studies of cross-linking reaction on chitosan fiber with glyoxal. *Carbohydrate Polymers*, *9*, 205–210.

Zeng, X., & Ruckenstein, E. (1996). Trypsin purification by p-aminobenzamidine immobilized on macroporous chitosan membranes. *Industrial and Engineering Chemistry Research*, *35*, 4169–4175.